CRL4RBBP7 is required for efficient CENP-A deposition at centromeres

Mouysset, Julien; Gilberto, Samuel; Meier, Michelle; Lampert, Fabienne; Belwal, Mukta; Meraldi, Patrick; Peter, Matthias

How to cite

MOUYSSET, Julien et al. CRL4RBBP7 is required for efficient CENP-A deposition at centromeres. In: Journal of cell science, 2015, vol. 128, n° 9, p. 1732–1745. doi: 10.1242/jcs.162305

This publication URL: https://archive-ouverte.unige.ch//unige:74214
Publication DOI: 10.1242/jcs.162305

© 2015. Published by The Company of Biologists Ltd | Journal of Cell Science (2015) 128, 1732–1745 doi:10.1242/jcs.162305

RESEARCH ARTICLE

CRL4^{RBBP7} is required for efficient CENP-A deposition at centromeres

Julien Mouysset[1,*], Samuel Gilberto[1,*], Michelle G. Meier[1,2], Fabienne Lampert[1], Mukta Belwal[1], Patrick Meraldi[1,2] and Matthias Peter[1,‡]

ABSTRACT

The mitotic spindle drives chromosome movement during mitosis and attaches to chromosomes at dedicated genomic loci named centromeres. Centromeres are epigenetically specified by their histone composition, namely the presence of the histone H3 variant CENP-A, which is regulated during the cell cycle by its dynamic expression and localization. Here, we combined biochemical methods and quantitative imaging approaches to investigate a new function of CUL4-RING E3 ubiquitin ligases (CRL4) in regulating CENP-A dynamics. We found that the core components CUL4 and DDB1 are required for centromeric loading of CENP-A, but do not influence CENP-A maintenance or pre-nucleosomal CENP-A levels. Interestingly, we identified RBBP7 as a substrate-specific CRL4 adaptor required for this process, in addition to its role in binding and stabilizing soluble CENP-A. Our data thus suggest that the CRL4 complex containing RBBP7 (CRL4^{RBBP7}) might regulate mitosis by promoting ubiquitin-dependent loading of newly synthesized CENP-A during the G1 phase of the cell cycle.

KEY WORDS: Centromere, Cullin, CENP-A, RBBP7

INTRODUCTION

During mitosis, replicated genetic material is faithfully and equally segregated between the two daughter cells. In order to achieve chromosomal segregation, microtubules emanating from the spindle are bound to chromosomes at specific genomic loci called centromeres (Westhorpe and Straight, 2013). Spindle dynamics then drive chromosome movement and separation (Walczak et al., 2010).

Except for in budding yeast, eukaryotic centromeres are not defined by a particular DNA sequence, but by an array of specific nucleosomes containing the histone H3 variant centromere protein-A (CENP-A, also known as CenH3) that replaces the canonical histone H3.1 variant (Ekwall, 2007). CENP-A nucleosomes are interspersed with H3.1-containing nucleosomes at the inner region of centromeres (Blower et al., 2002; Ribeiro et al., 2010; Sullivan and Karpen, 2004). CENP-A is required for the assembly of a large multi-protein complex, the kinetochore, which forms the interface between chromatin and the spindle (Westhorpe and Straight, 2013). Loss of CENP-A results in errors during chromosome congression and segregation, which are a source of genomic instability (Régnier et al., 2005). Beside its structural function, CENP-A is strictly and constitutively associated with the centromere, thus serving as an epigenetic marker of these loci (Allshire and Karpen, 2008; Fachinetti et al., 2013; Jansen et al., 2007; Schuh et al., 2007).

CENP-A protein levels and localization are stringently cell-cycle-regulated by mechanisms that are uncoupled from DNA replication (Jansen et al., 2007; Schuh et al., 2007), during which time centromeric CENP-A is diluted twofold (Hemmerich et al., 2008; Jansen et al., 2007; Mellone et al., 2011). CENP-A expression peaks during the G2 phase and its protein level is tightly regulated, possibly to avoid non-centromeric incorporation (Fachinetti et al., 2013; Lacoste et al., 2014).

The CENP-A-specific histone chaperone Holliday junction recognition protein (HJURP) is expressed concomitantly with CENP-A and is found associated with soluble pre-nucleosomal CENP-A (Bodor et al., 2013; Dunleavy et al., 2009; Foltz et al., 2009; Shuaib et al., 2010). HJURP is known to function in pre-nucleosomal CENP-A stabilization and in centromere deposition, by a mechanism that requires its dimerization (Zasadzińska et al., 2013), its binding to Mis18β (also known as OIP5) (Wang et al., 2014) and its DNA-binding activities (Müller et al., 2014). HJURP specifically recognizes CENP-A by interacting with the centromere-targeting domain (CATD; Black et al., 2007) of CENP-A to protect it from proteolysis (Foltz et al., 2009). HJURP is also responsible for the replenishment of the CENP-A pool (Dunleavy et al., 2011; Foltz et al., 2009; Kato et al., 2007) and for targeting the histone variant to centromeres during G1 (Jansen et al., 2007; Lagana et al., 2010; Moree et al., 2011).

In the early stage of CENP-A deposition, CENP-C, which connects centromeres to kinetochores, recruits Mis18BP1 and HJURP to centromeres and localizes itself at these genomic loci in a CENP-A-dependent manner (Barnhart et al., 2011; Carroll et al., 2010; Dambacher et al., 2012; Moree et al., 2011). Subsequently, in a positive-feedback loop, Mis18BP1 recruits additional CENP-A to centromeres (Barnhart et al., 2011). CDK1 inactivation in late mitosis and during G1 allows HJURP to associate with the centromere and to incorporate CENP-A (Müller et al., 2014; Silva et al., 2012). In early G1, CENP-A incorporation is facilitated by the remodelling and spacing factor complex, which associates with centromeres and is required for CENP-A retention (Perpelescu et al., 2009). In late G1, the small GTPase MgcRacGAP associates with centromeres and, through a GTP switch, stabilises freshly incorporated CENP-A (Lagana et al., 2010).

Additional factors seem important for chaperoning CENP-A. Retinoblastoma-binding protein 7 (RBBP7) and retinoblastoma-binding protein 4 (RBBP4) (also known as RbAp46 and RbAp48,

[1]Department of Biology, Institute of Biochemistry, Swiss Federal Institute of Technology, 8093 Zurich, Switzerland. [2]Department of Physiology and Metabolism, Faculty of Medicine, University of Geneva, 1211 Geneva, Switzerland.
*These authors contributed equally to this work

‡Author for correspondence (matthias.peter@bc.biol.ethz.ch)

Received 24 August 2014; Accepted 13 March 2015

respectively) are histone chaperones that are part of different chromatin modifier complexes such as the nucleosome remodelling and deacetylase complex, the Sin3-histone deacetylase complex, the polycomb repressive complex 2 or the nucleosome remodelling factor complex (Loyola and Almouzni, 2004). RBBP7 and RBBP4 interact with the N-terminal part of histone H4 (Murzina et al., 2008; Saade et al., 2009). It has been shown in fission yeast that the single RBBP7 and RBBP4 ortholog, Mis16, localizes to centromeres and is essential for CENP-A/Cnp1 centromeric localization and influences the acetylation status of centromeric regions (Hayashi et al., 2004). Experiments in human cells have revealed that RBBP7 and RBBP4 are required for CENP-A pre-nucleosomal stability (Dunleavy et al., 2009), therefore their depletion leads to a reduction in levels of CENP-A at centromeres (Hayashi et al., 2004).

Excess soluble CENP-A that is not associated with HJURP is degraded by the ubiquitin-proteasome system (UPS). The UPS consists of the sequential action of multiple enzymes that ultimately catalyse the transfer and covalent attachment of ubiquitin moieties to substrate proteins, terminating with the action of an E3 ubiquitin ligase (Pickart, 2004). In budding yeast, Psh1 has been identified as an E3 ubiquitin ligase targeting CENP-A/Cse4 for degradation by competing with HJURP for interaction with the CATD domain of CENP-A/Cse4 (Hewawasam et al., 2010; Ranjitkar et al., 2010). In fruit flies, a Skp1-cullin-F-box (SCF) E3 ubiquitin ligase containing Ppa (SCF^{Ppa}) has been suggested to regulate CENP-A/CID levels by a similar mechanism involving CATD recognition (Moreno-Moreno et al., 2011). SCF ubiquitin ligases belong to the large cullin–RING ligases (CRL) family, in which distinct cullin subunits function as scaffolding elements to assemble multi-protein complexes (Hotton and Callis, 2008). The core CUL4-based complex (CRL4) is CUL4–DDB1–RBX1 (with either CUL4A or CUL4B), where DDB1 bridges the association between CUL4A or CUL4B and substrate receptors. Substrate receptors for CRL4 complexes usually contain specific WD40 repeats and have been termed DDB1- and CUL4-associated factors (DCAF) (Lee and Zhou, 2007). CRL4 complexes are involved in different cellular processes, including DNA repair, DNA replication and chromatin remodelling (O'Connell and Harper, 2007).

Here, we propose a new role for CRL4, together with RBBP7 as a substrate specific receptor, in CENP-A centromeric deposition. Using an automated quantitative image analysis pipeline and biochemical approaches, we found that CUL4–DDB1 and RBBP7 form a stable complex (denoted $CRL4^{RBBP7}$) that is required for the deposition of CENP-A at centromeres. Moreover, RBBP7, but not the CRL4 complex, was necessary to protect the pre-nucleosomal fraction of CENP-A from proteolysis. Taken together, our data suggest that RBBP7 not only stabilizes soluble CENP-A, but, in complex with CRL4, also promotes loading of newly synthesized CENP-A at centromeres.

RESULTS

RBBP7 is required to stabilize CENP-A protein levels

To investigate the functional importance of CUL4 substrate receptors for mitosis, the duration of distinct mitotic stages was quantified by automated time-lapse imaging of HeLa cells expressing the chromatin marker histone-H2B–mCherry in which DCAFs were targeted by small interfering RNA (siRNA) (Held et al., 2010; Piwko et al., 2010). Interestingly, this analysis revealed that downregulation of RBBP7 (denoted siRBBP7) causes a prolonged metaphase-to-anaphase transition (Fig. 1A; supplementary material Fig. S1), resulting in an enrichment of mitotic cells as visualized by staining for phosphorylated histone H3. In contrast, we did not observe such mitotic defects in RBBP4-downregulated cells (denoted siRBBP4) (supplementary material Fig. S1), implying that RBBP7 is specifically required for timely progression through mitosis.

RBBP7 and RBBP4 are WD40-containing proteins that share almost 90% protein sequence identity, and are considered to represent the human orthologs of fission yeast Mis16, which is essential for CENP-A protein stability and centromeric association (Hayashi et al., 2004). We thus examined CENP-A protein levels in whole-cell extracts prepared from asynchronous HeLa cells after downregulation of RBBP4 and RBBP7 by siRNA (Fig. 1B). Indeed, CENP-A levels were reduced in HeLa cells lacking RBBP7 and both RBBP7 and RBBP4, similar to cells downregulated for the CENP-A-specific histone chaperone HJURP (Dunleavy et al., 2009). Because CENP-A levels fluctuate through the cell cycle (Stellfox et al., 2013), we performed a similar experiment in cells synchronized at the G1/S transition by double thymidine block release (DTBR) treatment. In contrast to siRBBP4, siRBBP7 treatment was sufficient to reduce CENP-A and HJURP protein levels (Fig. 1C,D), implying that RBBP7 stabilizes CENP-A through a cell-cycle-independent mechanism, possibly by regulating HJURP levels.

To address whether both cytosolic and chromatin-bound CENP-A pools were destabilized following RBBP7 depletion, whole-cell extracts were separated into cytosolic and chromatin fractions (Fig. 1E). As expected, CENP-A was enriched in chromatin fractions (siControl lanes). RBBP7 and RBBP4 were found in the cytosol and associated with chromatin, which is characteristic for components of chromatin modification complexes and histone chaperones (Loyola and Almouzni, 2004). Unfortunately, we could not address the role of RBBP4 in CENP-A chromatin association, as we failed to efficiently downregulate chromatin-bound RBBP4. We therefore observed that siRBBP7 decreased CENP-A levels in both the cytosol and chromatin fractions (Fig. 1E), whereas siRBBP4 reduced cytosolic CENP-A. We conclude that RBBP7 is required for CENP-A stabilization and chromatin association, possibly in cooperation with RBBP4. As expected, CENP-A levels were also decreased in whole-cell extracts prepared from G1/S synchronized cells downregulated for HJURP (Fig. 1F) (Dunleavy et al., 2009; Foltz et al., 2009). It is noteworthy that chromatin-associated HJURP seems to be mildly affected after 72 h of siRNA treatment. Based on these cell fractionation experiments, we conclude that RBBP7, RBBP4 and HJURP are required for stabilizing soluble CENP-A, and RBBP7 and HJURP also affect efficient CENP-A chromatin deposition. However, because these CENP-A pools are linked, we cannot exclude that the latter observation might be an indirect consequence of the reduced cytoplasmic CENP-A levels.

Association of CENP-A with centromeres requires RBBP7 and HJURP

As CENP-A chromatin association is restricted to centromeric loci (Allshire and Karpen, 2008), we next developed a microscopy-based experimental pipeline that allowed automated analysis of thousands of centromeres (Fig. 2A,B). Briefly, frames from fixed cells stained with appropriate antibodies were analysed using CellProfiler software (Carpenter et al., 2006), which allows the segmentation of cell nuclei and the quantification of pixel intensity values from centromeres with a high level of confidence (Fig. 2B; supplementary material Fig. S2A–D). To assess the cell cycle stage of individual cells, we used antibodies against cyclin A as a marker

Journal of Cell Science (2015) 128, 1732–1745 doi:10.1242/jcs.162305

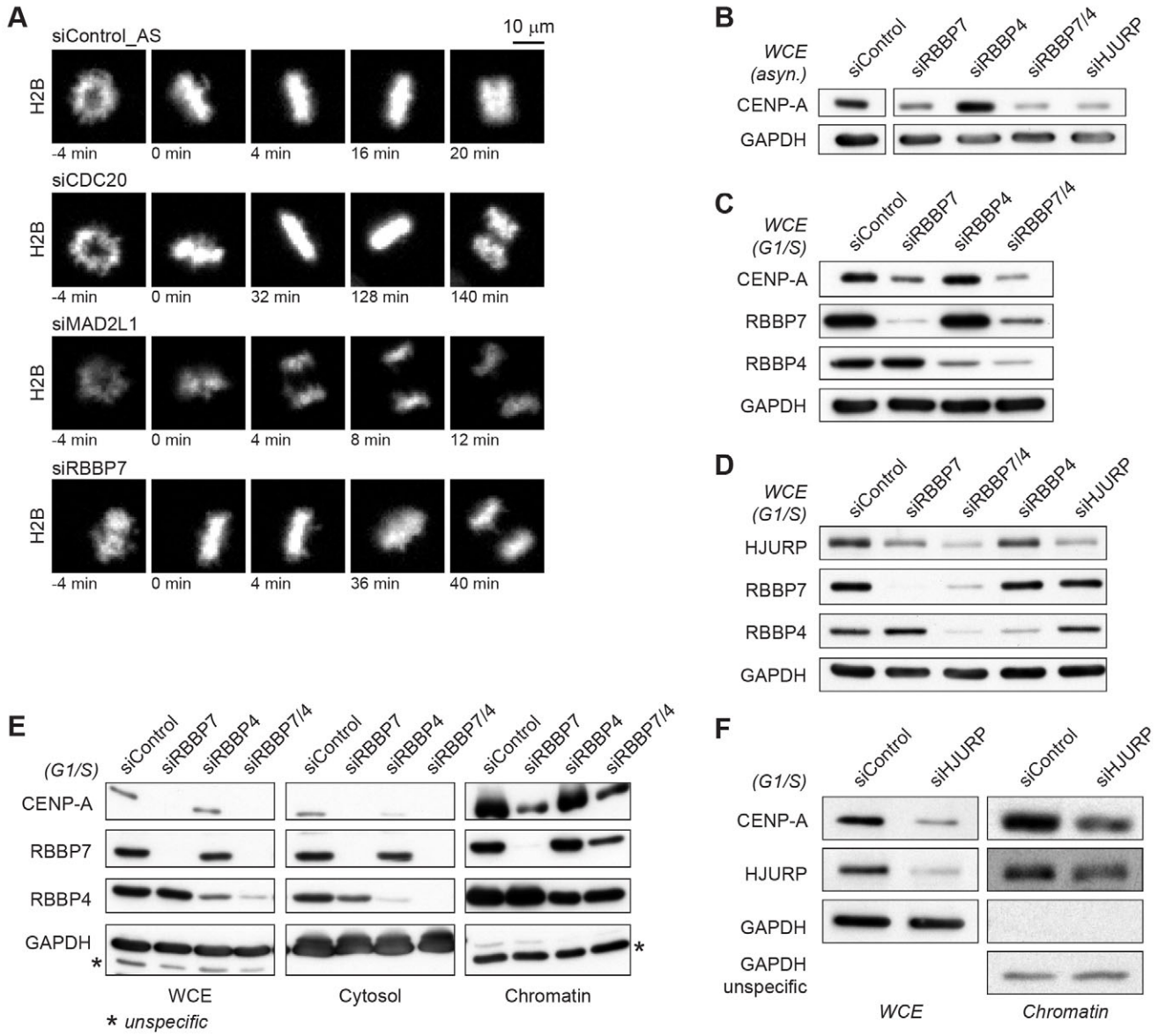

Fig. 1. RBBP7 regulates mitosis and is required to stabilize CENP-A protein levels. (A) Representative stills from time-lapse microscopy taken from a HeLa cell line expressing the chromatin marker histone-H2B–mCherry after treatment with the indicated siRNA. Time 0 min corresponds to the first still image displaying a metaphase plate morphology. Qiagen AllStar negative control (siControl_AS) is included, as well as controls for extended (siCDC20) and reduced (siMAD2L1) metaphase timing. (B–D) Western blot analyses from whole-cell extracts (WCE) from HeLa cells treated with the indicated siRNA that are in asynchronous culture (asyn.) (B) or had been synchronized at the G1/S transition by DTBR (C,D). Glyceraldehyde 3-phosphate dehydrogenase (GAPDH) was used as a loading control. (E,F) Western blot analyses from cell fractionation experiments of HeLa cells synchronized at the G1/S transition by DTBR treatment. GAPDH and a non-specific anti-GAPDH band were used as loading controls for the cytoplasmic and the chromatin fractions, respectively. siRBBP7/4 indicates treatment with siRNA against both RBBP7 and RBBP4.

of the G1/S transition (Fig. 2B). To validate this *in silico* synchronization method, we compared single-cell cyclin A values from asynchronous and synchronized cell populations, and observed that the mean nuclei pixel intensity of cyclin A in DTBR-synchronized cells changed the distribution of the measured values from a bimodal to a Gaussian distribution (supplementary material Fig. S2A,B). Based on the cyclin A staining, the total number of G1/S cells in an asynchronous population was ~14% (supplementary material Fig. S2A). To facilitate the analysis, we developed a library of in-house MATLAB scripts to extract various parameters from the CellProfiler data files including CENP-A maximum pixel intensities, centromere coordinates, nuclear cyclin A pixel intensity, nucleus coordinates and nucleus–centromere affiliations. The efficiency of centromere detection was compared by quantifying the same image dataset with our automated pipeline and with a semi-automated quantification protocol using Imaris software (Bitplane). The overall number of detected centromeres as well as the maximum pixel intensity distribution between the two methods was similar with 3369 spots detected with Imaris software versus 3473 spots detected with our analysis pipeline (supplementary material Fig. S2C). Moreover, manual validation of centromere detection revealed that the analysis pipeline

Journal of Cell Science (2015) 128, 1732–1745 doi:10.1242/jcs.162305

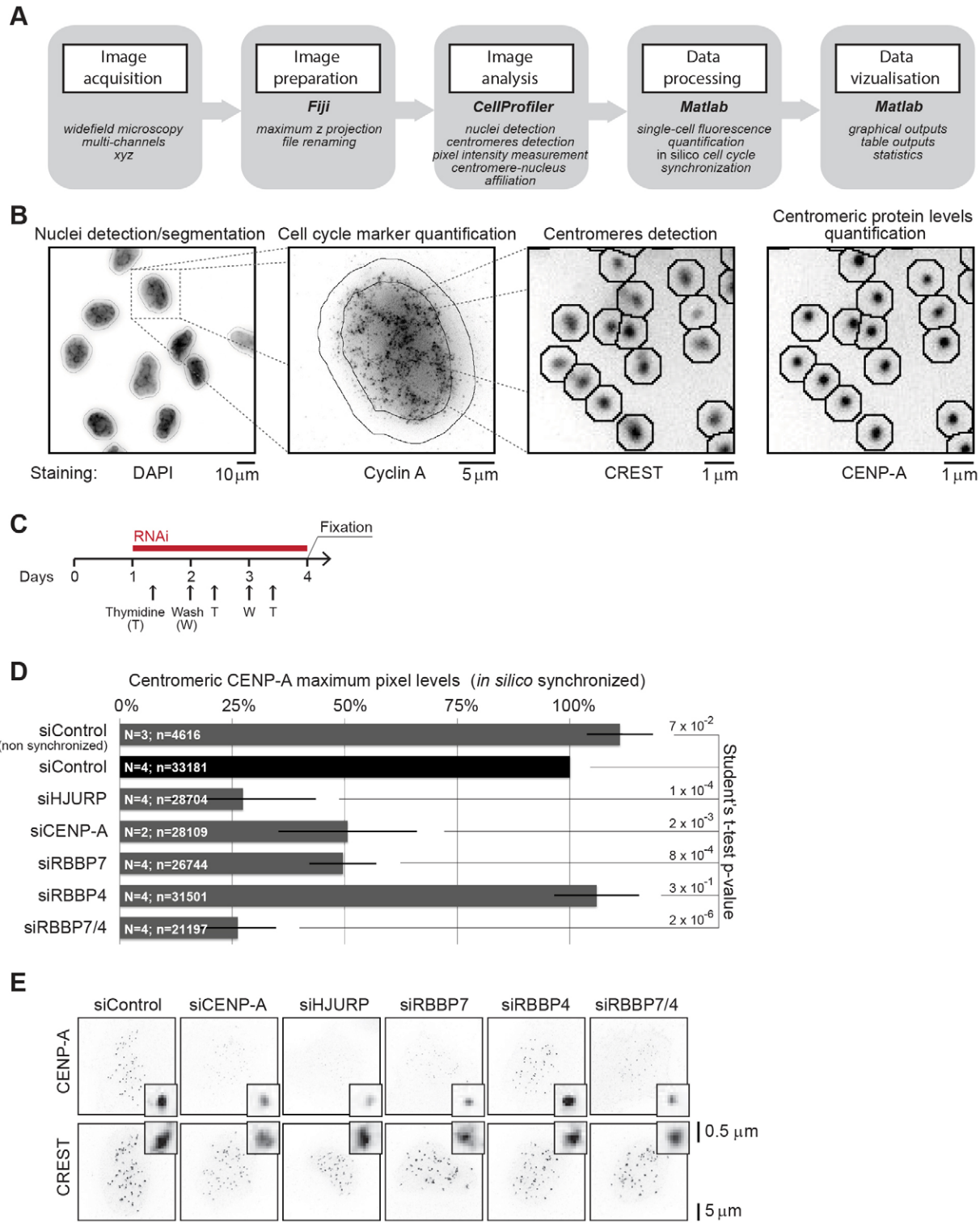

Fig. 2. RBBP7 is required for CENP-A centromeric association. (A) Schematic of the automated imaging pipeline workflow to quantify centromeric fluorescence. (B) Image analysis showing representative examples of CellProfiler image outputs. An example of each channel with use description is shown. (C) Timeline for cell handling prior to imaging to quantify endogenous CENP-A. (D) Quantification of centromeric CENP-A maximum pixel levels in DTBR-synchronized HeLa cells treated with the indicated siRNA normalized to those in siControl. *In silico* synchronization ensures that only cells at the G1/S transition were quantified, thus excluding cells that arrested in the cell cycle due to siRNA treatment or experimental conditions. 'N' represents the number of replicates, and 'n' the number of measured centromeres. Results are mean±s.d. *P*-values from a Wilcoxon rank sum test are indicated for each condition. siRBBP7/4 indicates treatment with siRNA against both RBBP7 and RBBP4. (E) Representative images for centromeric CENP-A protein levels from the quantitative analysis shown in D. A single nucleus and a representative centromere (inset) is shown per condition.

correctly assigned over 92% of the centromeres that were identified by manual counting (supplementary material Fig. S2D). Taken together, these data demonstrate that the established image-based centromere detection protocol is reliable and efficient, thus allowing quantification of a large number of centromeric fluorescent signals in an automated and unbiased fashion.

To examine whether RBBP7, RBBP4 and HJURP are required to regulate CENP-A levels at centromeres, HeLa cells were synchronized by DTBR at the G1/S transition (Fig. 2C; supplementary material Fig. S2E), which corresponds to the cell stage when most of the CENP-A molecules have been loaded at centromeres (Jansen et al., 2007), but have not yet been diluted during DNA replication (Stellfox et al., 2013). The cells were fixed 72 h after siRNA treatment to downregulate RBBP7, RBBP4 or HJURP (Fig. 2C), and centromeric CENP-A levels were quantified using the image-based analysis platform described above. For each experiment, DTBR synchronization and the siRNA-mediated knockdown efficiency were additionally monitored in parallel with the immunofluorescence staining (supplementary material Fig. S2E,F). As expected (Dunleavy et al., 2009; Foltz et al., 2009), siRNA against HJURP and CENP-A treatments significantly reduced centromeric CENP-A levels (Fig. 2D,E). Importantly, we also observed that siRBBP7, but not siRBBP4, led to a decrease of centromeric CENP-A (Fig. 2D,E). Treatment with siRNA against both RBBP7 and RBBP4 led to an even stronger reduction of centromeric CENP-A compared to the single RBBP7 downregulation, consistent with previous results (Hayashi et al., 2004). Taken together, these results confirm our cell fractionation experiments, and suggest that RBBP7 and RBBP4 cooperate to load and/or maintain CENP-A at centromeres.

RBBP7 and RBBP4 directly interact with DDB1

Although RBBP7 and RBBP4 lack the characteristic helix-loop-helix motif mediating the interaction with DDB1 (Fischer et al., 2011), they have been previously proposed to function as substrate receptors in CRL4 E3 ligase complexes (He et al., 2006). To confirm this observation, we immunoprecipitated endogenous CUL4A from extracts prepared from HeLa cells using specific anti-CUL4A antibodies. Like DDB1, RBBP7 was readily detected in CUL4A immunoprecipitates (Fig. 3A), demonstrating that the two proteins interact under physiological conditions. Importantly, binding between CUL4A and RBBP7 was reduced upon DDB1 depletion, supporting the notion that DDB1 links the two proteins *in vivo*. Conversely, N-terminally HA–2×Strep-tagged RBBP7 ectopically overexpressed in HeLa cells was able to co-precipitate endogenous DDB1 and RBBP4 (Fig. 3B). Thus, it appears that RBBP7 and RBBP4 stably associate with the known CRL4 core components, and are likely to function as genuine subunits of the complex. To substantiate these findings, we co-expressed RBBP7, DDB1 and RBX1 with either FLAG-tagged CUL4A or FLAG–CUL4B in insect cells. Importantly, we obtained a stable heterotetrameric complex after specific elution with 3×FLAG peptide (Fig. 3C), demonstrating that RBBP7 assembles into stable CRL4 complexes *in vitro*.

These experiments also indicate that RBBP4 and RBBP7 interact with each other, possibly forming homodimers or heterodimers, as it has been shown for multiple CRL-substrate-specific receptors. To corroborate these findings and further determine whether both RBBP7 and RBBP4 directly interact with DDB1, we co-expressed recombinant His-tagged DDB1 with either Strep-tagged RBBP7 or RBBP4 in insect cells, and performed Strep- or His-pull downs, respectively. Interestingly, we observed that RBBP7 and RBBP4 were able to co-purify with DDB1, indicating that there is a direct interaction (Fig. 3D,E). Thus, we conclude that RBBP7 and RBBP4 assemble *in vivo* and *in vitro* in a manner analogous to that shown by known substrate-specific receptors of CRL4 complexes (Fig. 3F).

CRL4 is required for centromeric association but not stability of CENP-A

We next investigated the requirement of CUL4 and DDB1 in CENP-A protein stability and centromeric association. In contrast to RBBP7 and RBBP4, total CENP-A protein levels were unaffected after simultaneous downregulation of both CUL4A and CUL4B using two distinct siRNAs (referred to hereafter as siCUL4A/B) or siRNA against DDB1 (denoted siDDB1) either in asynchronous cell populations (Fig. 4A) or in cells synchronized at the G1/S transition by a DTBR protocol (Fig. 4C). Likewise, siCUL4A/B and siDDB1 treatment did not alter HJURP levels. Cell fractionation experiments confirmed that, like CENP-A, a fraction of CUL4A, CUL4B and DDB1 associated with chromatin in cells synchronized at the G1/S transition (Fig. 4B; Obuse et al., 2004), consistent with the notion that CRL4 regulates chromatin-associated processes (O'Connell and Harper, 2007). Interestingly, CENP-A levels were decreased in the chromatin fraction of cells lacking DDB1 and to a lesser extent also in cells lacking CUL4A/B (Fig. 4C), suggesting that CRL4 modulates chromatin association and/or maintenance of CENP-A without affecting the stability of soluble CENP-A.

To support these data, we measured centromeric CENP-A protein levels using our quantitative automated imaging-based assay (Fig. 2A). Cells were treated as outlined in Fig. 2C, and DTBR synchronization and siRNA knockdown efficiency were monitored (supplementary material Fig. S2G,H). Consistently, we observed that centromeric CENP-A levels were reduced in DDB1-downregulated cells (67%±8, mean±s.d.) and also in CUL4A/B-downregulated cells, although not in a statistically significant manner (87%±12) (Fig. 4D,E). The reduction of centromeric CENP-A in siDDB1-treated cells was less pronounced compared to cells lacking siRBBP7 (30% as opposed to 50%, respectively), possibly because RBBP7, but not DDB1, also plays a role in stabilizing soluble CENP-A.

$CRL4^{RBBP7}$ is required to deposit newly synthesized CENP-A at centromeres

To examine whether RBBP7 in a complex with CRL4 is specifically required to load newly synthesized CENP-A molecules onto centromeres during G1, we performed CENP-A-loading experiments using the SNAP-tag labelling technology (Bodor et al., 2012; Jansen et al., 2007). To this end, we synchronized SNAP–CENP-A-expressing HeLa cells at the G1/S transition by DTBR prior to quenching of the SNAP-tag by the addition of bromothenylpteridine (Fig. 5A). The cells were released to allow translation of new SNAP–CENP-A protein, and thymidine was added again during this chase period to block the next G1/S transition. Before fixation, cells were fluorescently pulse-labelled with the SNAP-reactive TMR-Star reagent, thus ensuring that only SNAP–CENP-A protein produced after quenching is fluorescent (referred to as 'new CENP-A'). Although the efficiency of the quenching, chasing and labelling steps were carefully tested and optimized (supplementary material Fig. S3A,B), the dynamic range of the SNAP signal was too weak to allow a reliable automated analysis. We thus quantified manually the proportion of cells that

Journal of Cell Science (2015) 128, 1732–1745 doi:10.1242/jcs.162305

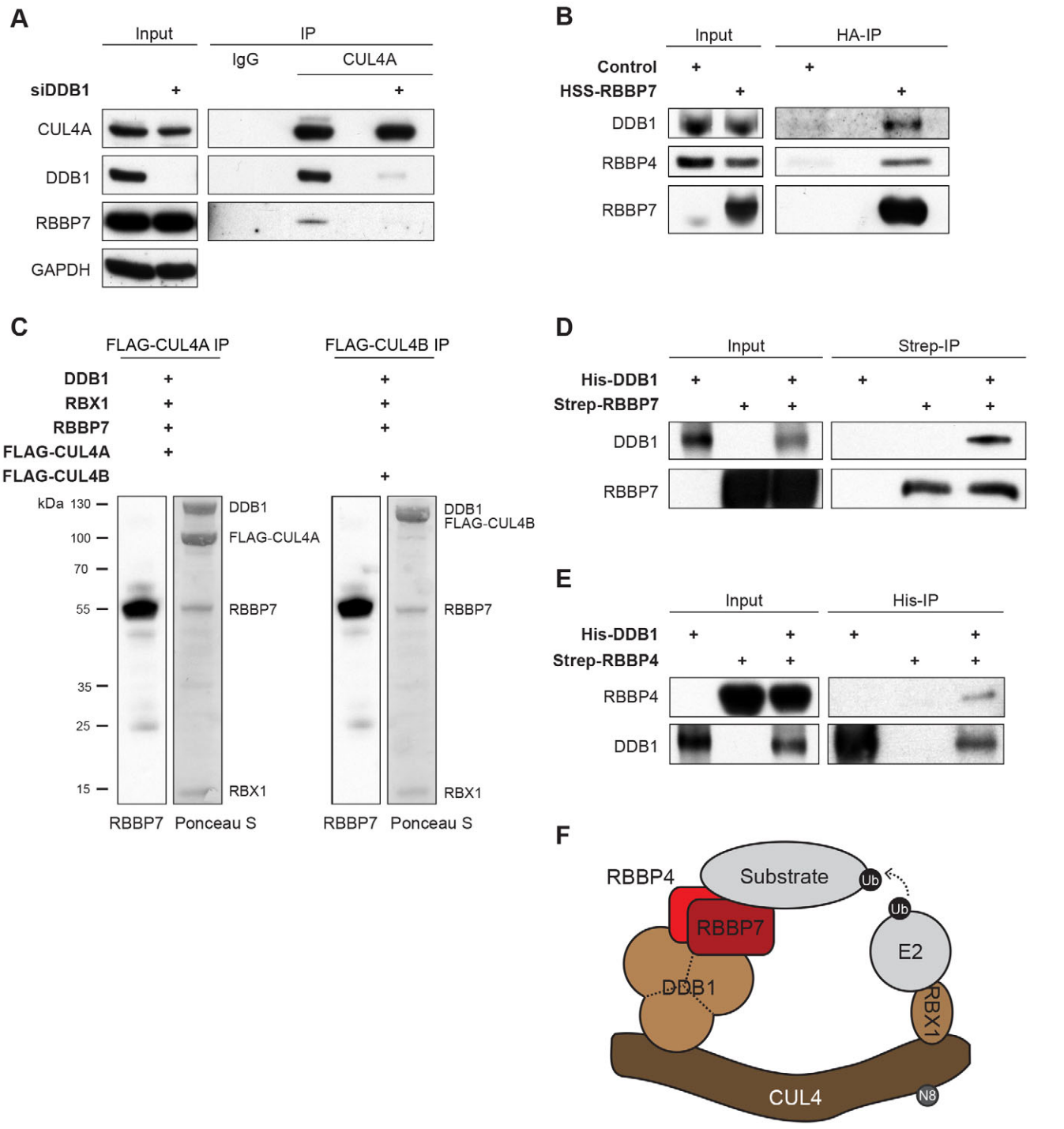

Fig. 3. RBBP7 and RBBP4 interact with DDB1 *in vivo* and *in vitro*. (A) Immunoprecipitates (IP) of endogenous CUL4A from HeLa cell extracts using a rabbit anti-CUL4A antibody were analysed by western blotting, with or without depletion of DDB1 by siRNA (siDDB1). A non-specific immunoglobulin G (IgG) was also used as a negative control. (B) HeLa cells were transiently transfected with a HA–Strep–Strep–RBBP7 construct. Cell extracts were used for HA pulldown experiments and analysed by western blotting. Control conditions correspond to cells treated with transfection reagents without DNA. (C) DDB1, RBX1 and RBBP7 were co-expressed with either FLAG–CUL4A or FLAG–CUL4B in a single multibac vector in Sf-9 insect cells. CUL4 complexes were purified on a FLAG-antibody column, and eluted with 3×FLAG peptide. Co-precipitating proteins with CUL4A (left panels) and CUL4B (right panels) were visualized by Ponceau S staining (right lanes) and western blotting for RBBP7 (left lanes). (D,E) High Five insect cells were infected with His–DDB1, Strep–RBBP7 and Strep–RBBP4. Strep (D) or His pulldowns (E) were performed and analysed by western blotting. (F) Model for the $CRL4^{RBBP7–RBBP4}$ E3 ubiquitin ligase complex. Ub, ubiquitin; N8, Nedd8; E2, E2 ubiquitin-conjugating enzyme. The dotted arrow indicates ubiquitin transfer from the E2 enzyme to the bound protein substrate.

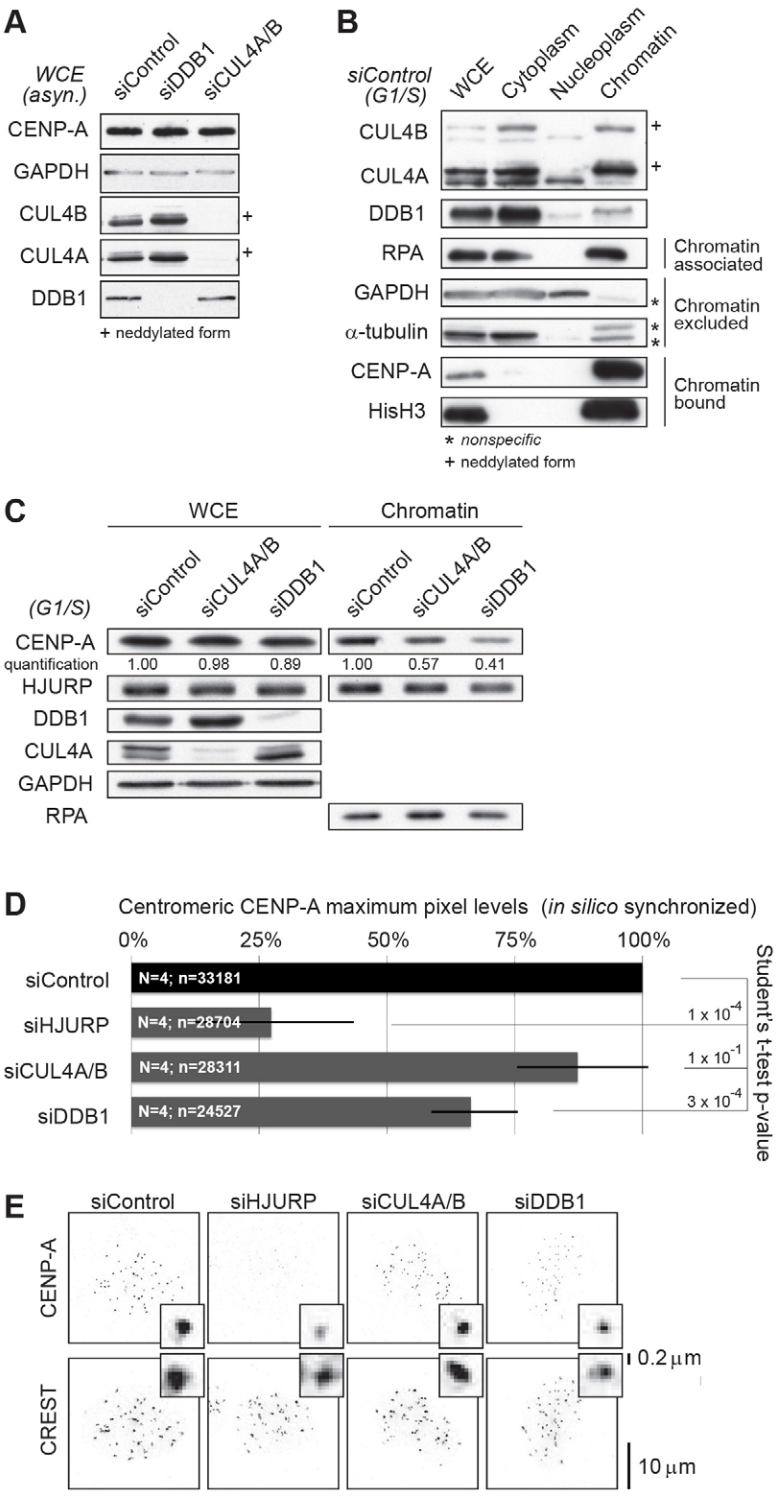

Fig. 4. Depletion of DDB1 reduces centromeric CENP-A association. (A,C) Western blot analyses of whole-cell extracts (WCE) prepared from non-synchronized (A) or DTBR-synchronized HeLa cells accumulating at the G1/S transition that had been treated with the indicated siRNA. In C, GAPDH and RPA was used as a loading control for WCE and the chromatin fraction, respectively. The intensity of the bands was quantified using Fiji software and normalized to the loading control. '+' marks the neddylated form of CUL4. (B) HeLa cells treated with siControl were synchronized at the G1/S transition by DTBR. Cells were lysed, separated into cytoplasmic, nuclear (chromatin excluded), and chromatin-bound fractions and analysed by western blotting with the indicated antibodies. '+' marks neddylated CUL4; '*' marks a nonspecific band. (D) Quantification of centromeric CENP-A maximum pixel levels in DTBR-synchronized HeLa cells treated with the indicated siRNA normalized to siControl. *In silico* synchronization based on cyclin A staining excludes the analysis of cells that arrested in the cell cycle due to siRNA treatment or experimental conditions. 'N' represents number of replicates, and 'n' the number of centromeres measured. Results are mean±s.d. *P*-values from a Wilcoxon rank sum test are indicated accordingly for each condition. (E) Representative images for centromeric CENP-A protein levels from the quantitative analysis as in D are shown. A single nucleus and a representative centromere (inset) is shown per condition. siCUL4A/B indicates treatment with siRNA against both CUL4A and CUL4B.

displayed fluorescent centromeric TMR-Star signals. As expected, we observed that siHJURP led to a complete absence of cells positive for centromeric fluorescent signal (Fig. 5B,C) (Foltz et al., 2009). Strikingly, siCUL4A/B, siDDB1 and siRBBP7 drastically impaired the loading of new CENP-A at centromeres (Fig. 5B,C), whereas siRBBP4 had no effect. Cell cycle analysis by flow-cytometry and immunofluorescence excluded the possibility that these strong defects were indirectly caused by cell cycle delays in cells lacking CUL4A/B (supplementary material Fig. S4A,B), although we observed a mild cell cycle delay in DDB1-depleted cells. These results thus uncover an important role of RBBP7 and the CRL4 core components in centromeric loading of CENP-A, and suggest that a $CRL4^{RBBP7}$-dependent ubiquitylation step is required for this process.

CENP-A is a variant belonging to the histone H3 family that is specifically assembled at centromeres (Allshire and Karpen,

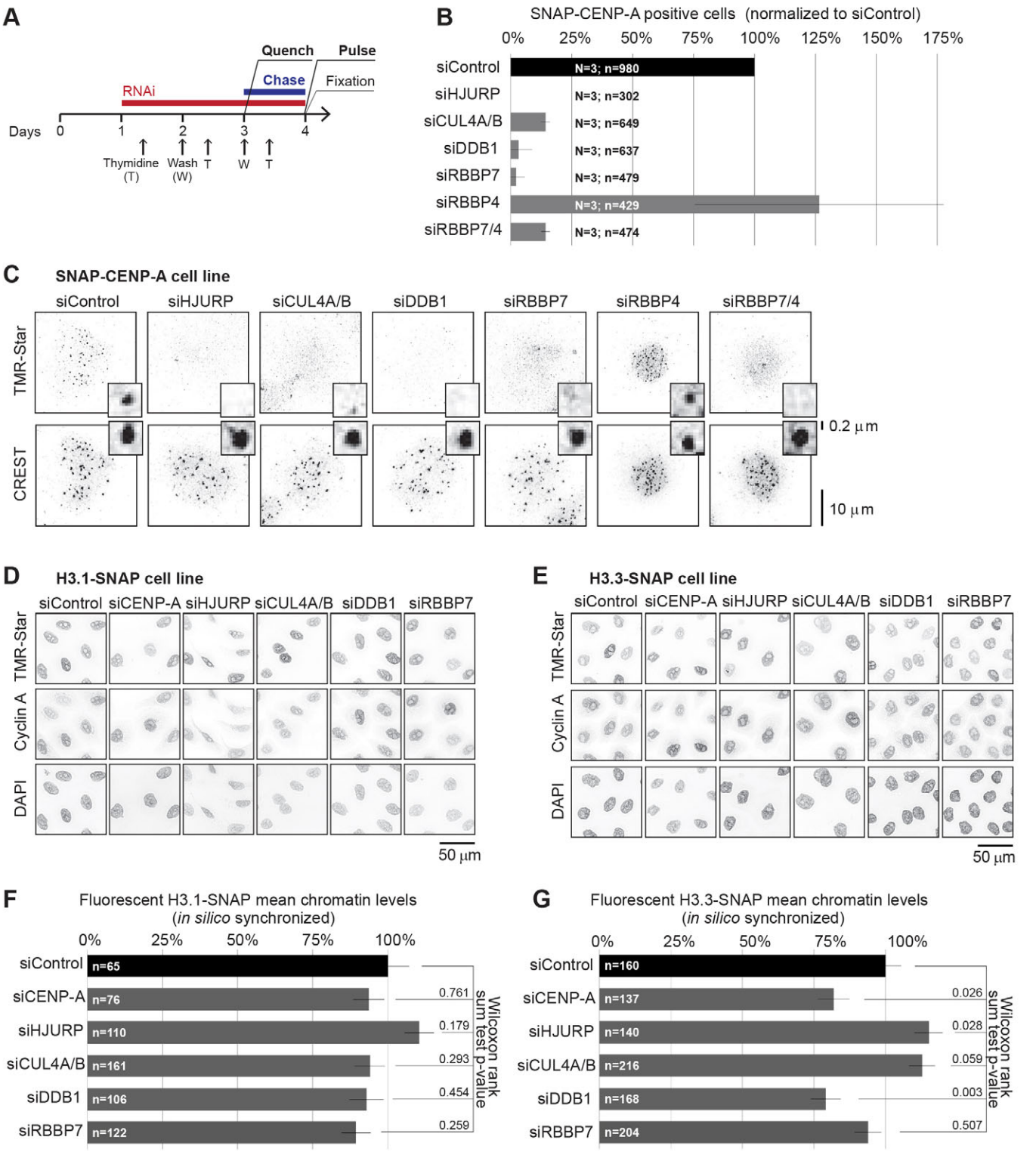

Fig. 5. CRL4^{RBBP7} is required to deposit CENP-A at centromeres. (A) Timeline of cell handling prior to imaging of the SNAP-histone loading assay. The SNAP-tag is quenched by the addition of bromothenylpteridine and TMR-Star allows SNAP–CENP-A fluorescence pulse-labelling. (B) Fluorescent centromeric TMR-Star-labelled SNAP-CENP-A nuclei were counted manually in cells depleted for the indicated proteins by siRNA, and normalized to control conditions. 'N' represents number of replicates, and 'n' is the number of nuclei counted. Results are mean±s.d. (C) Representative images of centromeric fluorescently labelled SNAP–CENP-A protein as in B are shown. A single nucleus and a representative centromere (inset) is shown per condition. (D,E) Representative images from HeLa cell lines expressing H3.1–SNAP (D) and H3.3–SNAP (E) from the quantitative analysis shown in F and G, respectively. Cells were treated as described in A. (F,G) Quantification of chromatin H3.1–SNAP (F) and H3.3–SNAP (G) maximum pixel levels in *in silico* synchronized HeLa cells. 'n' represents number of nuclei measured. Results are mean±s.e.m. *P*-values from a Wilcoxon rank sum test are indicated accordingly for each condition. siRBBP7/4 indicates treatment with siRNA against both RBBP7 and RBBP4; siCUL4A/B indicates treatment with siRNA against both CUL4A and CUL4B.

2008). Histone H3.1 represents the canonical histone H3, and its expression is dependent on DNA replication. Histone H3.3 denotes a non-DNA replication-dependent histone H3, which is incorporated into chromatin throughout the cell cycle at active transcription promoters, telomeres and centromeres (Biterge and Schneider, 2014; Tagami et al., 2004). We thus tested whether, like CENP-A, chromatin deposition of histones H3.1 and H3.3 also requires $CRL4^{RBBP7}$ activity. As described for CENP-A, we monitored the pool of 'new H3.1' and 'new H3.3' incorporated into chromatin after one complete cell cycle of HeLa cells expressing H3.1–SNAP or H3.3–SNAP transgenes (Ray-Gallet et al., 2011) synchronized at the G1/S transition (Fig. 5A). The efficiency of quenching, chasing and pulse labelling was optimized for both H3.1–SNAP and H3.3–SNAP cell lines (supplementary material Fig. S3C–F), and the mean nuclear TMR-Star fluorescence of both new H3.1 and new H3.3 histones was quantified with the automated image analysis pipeline for *in silico* synchronized cells as described in Fig. 2A. Interestingly, the mean nuclear levels of new H3.1 cells were unaffected in cells with downregulated CUL4A/B and DDB1 (Fig. 5D,F), whereas the loading of new H3.3 was unaffected by siCUL4A/B, but possibly slightly reduced after siDDB1 treatment (Fig. 5E,G). As expected, downregulation of HJURP had no effect on loading of the H3.1 and H3.3 variants, demonstrating the specificity of the assay. Based on these results, we conclude that $CRL4^{RBBP7}$ activity is required for efficient loading of CENP-A at centromeres, and that this function does not involve a general histone deposition function but rather a CENP-A-specific mechanism.

$CRL4^{RBBP7}$ is not required for maintaining loaded CENP-A at centromeres

CENP-A remains constitutively associated with centromeres throughout the cell cycle, and is only diluted by DNA replication and subsequently replenished after mitosis (Jansen et al., 2007). To test whether $CRL4^{RBBP7}$ is not only required to load but also to maintain CENP-A at centromeres, we followed the fate of centromeric CENP-A in a maintenance assay. To this end, synchronized HeLa cells expressing SNAP–CENP-A (Jansen et al., 2007) were fluorescently pulse labelled with TMR-Star (Fig. 6A), thereby specifically labelling SNAP–CENP-A that is expressed before the pulse labelling ('old CENP-A'). The dilution of 'old CENP-A' at centromeres was then quantified after different chasing periods ranging from 0 to 3 days using our automated imaging pipeline (Fig. 6A). With control siRNA, a progressive decrease of the old CENP-A centromeric signal was observed over the course of the chase period (Fig. 6B,C), with kinetics comparable to other published reports (Bodor et al., 2013; Fachinetti et al., 2013). Interestingly siRNA-mediated downregulation of CENP-A, CUL4A/B, DDB1 and RBBP7 resulted in decay kinetics similar to those with control siRNA (Fig. 6B,C), suggesting that $CRL4^{RBBP7}$ is not required for CENP-A maintenance at centromeres. To monitor proper cell cycle progression under the experimental conditions, we pulse labelled S-phase cells with BrdU 16 h before harvesting (supplementary material Fig. S4C). The appearance of BrdU-labelled cells in G1-phase demonstrates that all cells underwent mitosis, and the expected cell cycle delay was only observed for DDB1-depleted cells after a 72-h siRNA treatment. Taken together, these results suggest that the $CRL4^{RBBP7}$ E3 ubiquitin ligase complex is required to specifically load CENP-A on centromeres during the G1 phase, but is not involved in maintaining CENP-A on centromeres throughout the cell cycle.

DISCUSSION

CENP-A centromeric deposition has been described as a multi-step event that requires a priming phase, in which centromeres recruit specific factors, a deposition phase and a maintenance phase in order to stabilize freshly incorporated histones (Müller and Almouzni, 2014). In this study, we propose a new role for CUL4A/B–DDB1, together with RBBP7, in CENP-A centromeric deposition. Biochemical analysis showed that the levels of chromatin-bound CENP-A were reduced after downregulation of CUL4A/B, DDB1 and RBBP7, and microscopy-based assays identified defects in loading of CENP-A at centromeric locations. We showed that the $CRL4^{RBBP7}$ complex has no impact on other aspects of CENP-A dynamics such as pre-nucleosomal stabilization and centromeric localization maintenance. Importantly, siRNA against CUL4A/B, DDB1 and RBBP7 led to prolonged mitotic progression, reminiscent of the CENP-A homozygous knockout phenotype (Fachinetti et al., 2013). Our work thus suggests a new role for CRL4-based ubiquitin ligases in regulating centromeric loading of CENP-A during G1.

Automated image analysis quantifies levels and dynamics of CENP-A at individual centromeres

Automated processing of imaging data allows the analysis of large datasets, thereby facilitating extraction of multiple features and enabling consistent unbiased processing of various experimental conditions. In order to analyse the centromeric fluorescent signal, we developed a pipeline for in-depth automated image analysis by combining computer-assisted analysis with CellProfiler and MATLAB in-house scripts. We were able to analyse a large number of centromeres per nuclei on a single-cell basis, which was not possible with previous methods (Bodor et al., 2012). Validation revealed that the analysis pipeline detected over 92% of the centromeres, and allowed a quantification of the levels and distribution of proteins on single centromeres in an unbiased manner. Combined with appropriate cell cycle markers, this method not only permitted us to determine average numbers but also cell-to-cell and centromere-to-centromere variations. The image-based method will thus be of broad interest, and could also be adapted to analyse centromere dynamics in more complex samples such as 3D cultures or tissues. Finally, the developed image-processing pipeline could be applied to study other biological processes, including quantifying aneuploidy or the detection and quantification of other types of foci such as DNA damage markers (data not shown).

RBBP7 and RBBP4 are required to stabilize CENP-A and the histone chaperone HJURP *in vivo*

RBBP7 and RBBP4 are components of multiple chromatin modification complexes, and interact with histone target substrates (Loyola and Almouzni, 2004). In contrast to their counterpart in fission yeast, human RBBP7 and RBBP4 proteins are not enriched at centromeric regions, but are required for the stability and centromeric localization of CENP-A (Hayashi et al., 2004). It was shown previously that RBBP4 is associated with pre-nucleosomal CENP-A, and that RBBP7 and RBBP4 are required to stabilize the soluble fraction of the CENP-A-specific histone chaperone HJURP (Dunleavy et al., 2009). Our data confirm that RBBP7 and RBBP4 stabilize HJURP and pre-nucleosomal CENP-A, supporting a model in which RBBP7 and

Journal of Cell Science (2015) 128, 1732–1745 doi:10.1242/jcs.162305

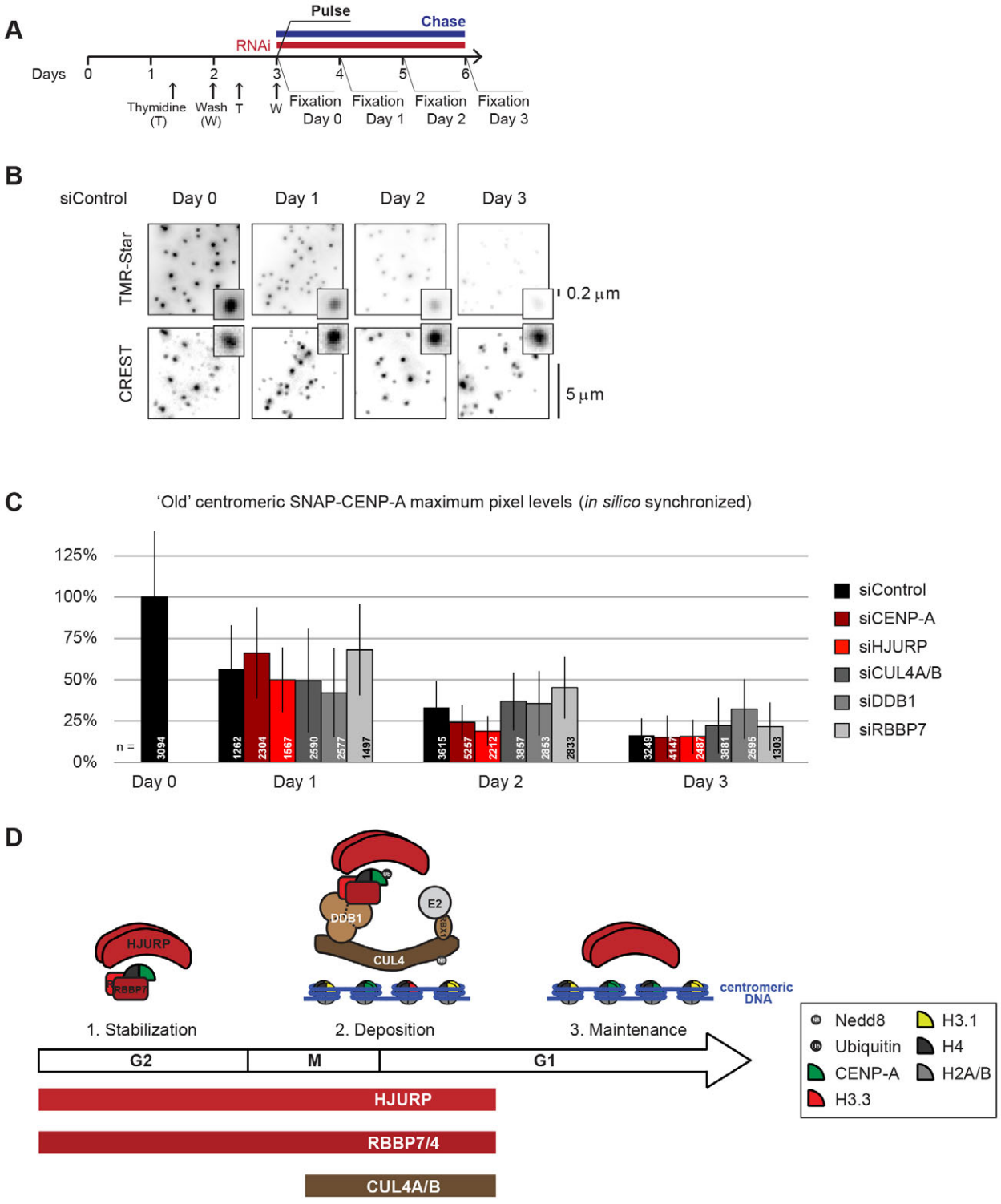

Fig. 6. CRL4^{RBBP7} is not required for centromeric CENP-A maintenance. (A) Timeline of cell handling prior to imaging of the SNAP–CENP-A maintenance assay. (B) Representative images of cells treated with siControl oligonucleotides show centromeric fluorescently labelled SNAP–CENP-A protein (upper row) after the indicated chase period (days). Staining with CREST antibodies was included as a control (lower row). (C) Quantification of centromeric SNAP-CENP-A maximum pixel levels normalized to siControl conditions in *in silico* synchronized HeLa cells treated with the indicated siRNA. 'n' represents the number of centromeres measured, and results are median±s.d. siCUL4A/B indicates treatment with siRNA against both CUL4A and CUL4B. (D) Model of the timing of HJURP, RBBP4 and RBBP7, and CRL4$^{RBBP7–RBBP4}$ activity in CENP-A dynamics. Our data suggest that CRL4$^{RBBP7–RBBP4}$-dependent ubiquitylation promotes CENP-A loading at the G1/S transition.

RBBP4 together with HJURP protect soluble CENP-A from proteolysis.

HJURP dimers recognize and stabilize the heterodimeric CENP-A–histone-H4 pre-nucleosomal complex by interacting with the CATD domain of CENP-A (Bassett et al., 2012; Foltz et al., 2009; Zasadzińska et al., 2013). Our data suggest that pre-nucleosomal CENP-A stabilization requires both RBBP7 and RBBP4, but that their functions are not redundant. RBBP4 directly interacts with histone H4 (Murzina et al., 2008; Saade et al., 2009) and colocalizes with pre-nucleosomal CENP-A (Dunleavy et al., 2009), suggesting that the pre-nucleosomal CENP-A complex is composed of a HJURP homodimer and RBBP7–RBBP4 and CENP-A–histone-H4 heterodimers (Fig. 6D). Recently, it has been shown that in fruit flies the CUL3-based complex $CRL3^{RDX}$ mono-ubiquitylates CENP-A/CID, which stabilizes CENP-A/CID and the HJURP ortholog CAL1 (Bade et al., 2014). Whether mammalian CRL3 similarly regulates the stability of CENP-A and/or HJURP remains to be determined.

CRL4 is required for efficient loading of new CENP-A to centromeres *in vivo*

In contrast to RBBP7 and RBBP4 downregulation, siCUL4A/B and siDDB1 do not lead to decreased levels of soluble CENP-A or HJURP. Instead, CUL4A/B and DDB1 appear to be specifically required for centromeric recruitment of CENP-A, without altering global CENP-A levels (Fig. 6D). Indeed, CUL4A and DDB1 are both present at centromeres during interphase (Obuse et al., 2004), and fractionation experiments revealed that the neddylated (active) forms of CUL4A and CUL4B are both enriched in the chromatin fraction at the G1/S transition (Fig. 4B), a point when pre-nucleosomal CENP-A is loaded on centromeres. Available evidence suggests that RBBP7 and RBBP4 function as substrate-specific adaptors in CRL4 complexes to load CENP-A. RBBP7 co-immunoprecipitates *in vivo* with CUL4A in a DDB1-dependent manner (Fig. 3A,B; He et al., 2006), and both RBBP7 and RBBP4 directly bind DDB1 *in vitro* in heterologous expression systems (Fig. 3C–E). Although a sequence motif search identified RBBP7 and RBBP4 as DDB1–CUL4A interactors possessing a DDB1-binding WD40 protein box, RBBP7 and RBBP4 lack the helix-loop-helix motif characteristic for established DCAFs, which mediates the interaction with DDB1 (Fischer et al., 2011). Nevertheless, we were able to reconstitute stable $CRL4^{RBBP7}$ complexes *in vitro*, and it will be interesting to analyse them structurally and measure their ubiquitylation activity on potential substrates.

Overall, our results suggest that RBBP7 and probably also RBBP4 act at two distinct stages in CENP-A dynamics: (1) during stabilization of pre-nucleosomal CENP-A and HJURP, and (2) during formation of a $CRL4^{RBBP7}$ complex at centromeres to deposit CENP-A at chromatin (Fig. 6D). Although total CENP-A levels were not altered in cells lacking any CRL4 core subunits, we cannot exclude that $CRL4^{RBBP7}$ affects CENP-A stability specifically during the deposition process. We could not fully investigate the involvement of RBBP4 for CENP-A loading due to its inefficient downregulation at chromatin. Nonetheless, given that RBBP4 also directly interacts with DDB1, it is likely that $CRL4^{RBBP4}$ and $CRL4^{RBBP7–RBBP4}$ complexes similarly promote CENP-A deposition on centromeres (Fig. 6D). Given that CRLs might dimerize to regulate their activity (Merlet et al., 2009), it is tempting to speculate that CRL4 recognizes the pre-nucleosomal CENP-A complex containing RBBP7 and RBBP4 and that $CRL4^{RBBP7}$–$CRL4^{RBBP4}$ heterodimers might be responsible for promoting CENP-A deposition. However, biochemical *in vitro* reconstitution assays will be necessary to test this exciting hypothesis.

CRL4 is not required to regulate deposition of other histone H3 variants *in vivo*

CENP-A is a variant of histone H3 that marks centromeric chromatin (Ekwall, 2007). Additional histone H3 variants have been described that as well as performing functions at centromeres also do so at other heterochromatic regions with unrelated functions (Biterge and Schneider, 2014). In contrast to CENP-A, by using quench-chase-pulse SNAP-tagged labelling we could not observe a defect in loading of the histone H3 variants H3.1 and H3.3 in cells downregulated for CUL4A/B, DDB1 and RBBP7, implying that $CRL4^{RBBP7}$ is specifically required for CENP-A deposition. Moreover, CENP-A, H3.1 and H3.3 maintenance at centromeres was independent of CUL4, DDB1 and RBBP7.

Interestingly, Rtt101, the functional budding yeast CUL4 ortholog (Zaidi et al., 2008), has recently been shown to be involved in histone dynamics by a conserved mechanism that involves CUL4A- and DDB1-dependent turnover of H3.1 and H3.3 (Han et al., 2013). Several aspects could explain the differences observed. First, we have experimentally synchronized the cells and monitored H3.1 and H3.3 dynamics at the same cell cycle stage. Second, we implemented a longer chase period to compare cells with a similar history regarding their cell cycle progression. Finally, we downregulated both CUL4A and CUL4B, not only CUL4A, to avoid compensatory mechanisms from these two very close paralogs. Taken together, our results suggest that $CRL4^{RBBP7}$ is primarily required for CENP-A deposition, and is not generally involved in histone dynamics.

What are the physiological $CRL4^{RBBP7}$ substrates for CENP-A deposition?

Our results indicate that CUL4 and DDB1 are required for CENP-A deposition at centromeres, most likely by forming an E3 ligase complex together with RBBP7. This raises many questions for future study. Clearly, it would be of prime interest to identify the crucial $CRL4^{RBBP7}$ substrates. Recent work in *Drosophila* has identified CENP-A as a potential candidate (Bade et al., 2014), and it is possible that ubiquitylation of newly synthesized CENP-A is required for its centromere deposition. Another line of questioning derives from the observation that centromeric regions are enriched in histone methylation and display a low degree of acetylation, which appears to influence the structural organization of chromatin (Bergmann et al., 2011; Kim et al., 2012; Ohzeki et al., 2012). Interestingly, the ortholog of RBBP7 and RBBP4 in fission yeast, Mis16, is necessary for maintaining the deacetylated status of centromeres (Hayashi et al., 2004). Therefore, the $CRL4^{RBBP7}$ complex might regulate the acetylation status of centromeric proteins, thereby promoting recruitment of the pre-nucleosomal CENP-A complex or other factors important for chromatin structure of centromeres. Because ubiquitylated substrates at least transiently interact with specific DCAFs, the search for proteins interacting with RBBP7 and RBBP4 may be a fruitful focus for future research.

MATERIALS AND METHODS

Cell culture, cell transfection, siRNAs and cell synchronization

HeLa cell lines were grown in a humidified incubator at 37°C and 5% CO_2 in Dulbecco's modified Eagle medium (DMEM, Gibco, Invitrogen, Carlsbad,

CA) supplemented with 10% fetal calf serum (FCS, PAA Laboratories) and 1% penicillin-streptomycin (Gibco). The stable SNAP–CENP-A-expressing cell line was produced by transfecting HeLa E1 cells with a pSEMS1-SV40-CENP-A plasmid using FUGENE6 reagents (Roche, Basel, Switzerland) according to the manufacturer's instructions. 5 mM puromycin (Gibco) and 2 mM blasticidin S (PAA Laboratories, GE Healthcare, Little Chalfont, UK) were used as selection antibiotics for HeLa SNAP–CENP-A and SNAP–H3.1 or SNAP–H3.3 cell lines (Ray-Gallet et al., 2011), respectively. HeLa 'Kyoto' cells stably expressing H2B–mCherry and IBB–mEGFP (IBB is the importin-β-binding domain of importin-α) (Held et al., 2010) were grown in 0.5 mg/ml geneticin (Calbiochem, Merck, Darmstadt, Germany) and 0.5 µg/ml puromycin (Gibco). DNA plasmid was transiently transfected using Lipofectamine 2000 (Invitrogen) according to the manufacturer's instructions. For RNAi experiments, cells were transfected with 50 nM siRNAs (Qiagen, Hilden, Germany or Microsynth, Balgach, Switzerland) for 72 h using Oligofectamine (Invitrogen) or Lipofectamine RNAiMAX (Invitrogen) according to the manufacturer's instructions. The target sequences of double-stranded RNA used in this study were as follows: siControl, 5′-GGACCTGGAGGTCTGCTGT-3′ (McHedlishvili et al., 2012); siCENP-A, 5′-AACACAGTCGGCGGAGACAAG-3′ (Carroll et al., 2009); siHJURP, 5′-CTACTGGGCTCAACTGCAA-3′ (Dunleavy et al., 2009); siCUL4A, 5′-AAGAATCCTACTGCTGATCGA-3′ (Piwko et al., 2010); siCUL4B, 5′-CACCGTCTCTAGCTTTGCTAA-3′ (Piwko et al., 2010); siDDB1, 5′-CCACTAGATCGCGATAATAAA-3′ (Piwko et al., 2010); siRBBP7, 5′-GCGGATAAGACCGTAGCTTTA-3′ (Piwko et al., 2010); siRBBP4, 5′-GCCACTCAGTTGATGCTCA-3′ (Hayashi et al., 2004); siCDC20, 5′-AACCTTGTGGATTGGAGTTCT-3′ (Piwko et al., 2010); and siMAD2L1, 5′-CAGAAAGCTATCCAGG-ATGAA-3′ (Piwko et al., 2010). Cells were synchronized at the G1/S transition by 16 h incubation in 2 mM thymidine (Sigma, St. Louis, MO), washed twice with pre-warmed phosphate-buffered saline (PBS) solution, incubated for 9 h in culture medium and then incubated for another 16 h in 2 mM thymidine.

Immunofluorescence, SNAP tag labelling and microscopy

Cells were fixed as described previously (McHedlishvili et al., 2012). The following antibodies were used: anti-CREST antisera (1:250, Antibodies Incorporated), rabbit anti-cyclin-A (1:500, Santa Cruz Biotechnology) and mouse anti-CENP-A (1:2000, Abcam, Cambridge, UK). Cross-absorbed fluorescently labelled antibodies were used (Invitrogen). SNAP-tag labelling was performed as described previously (Bodor et al., 2012; Jansen et al., 2007). For quenching, cells were incubated for 30 min in 2 µM bromothenylpteridine (New England Biolabs, Ipswich, MA) dissolved in culture medium followed by two washes with pre-warmed PBS, a 30-min incubation in culture medium and another wash with pre-warmed PBS. For pulse labelling, cells were incubated for 15 min in 2 µM TMR-Star (New England Biolabs) dissolved in culture medium followed by the same sequence of washes described above for the SNAP-tag quenching. Different chase timing was performed for the deposition and maintenance assays as depicted in Fig. 5A and Fig. 6A, respectively. *z*-stacks of cells were acquired in 0.2-µm z-steps over a 50 µm depth using a 100× oil (NA 1.4) UPlanSApo objective (Olympus, Shinjuku, Japan) with a Cell-R epifluorescence microscope (Olympus) mounted with a Orca ER camera (Hamamatsu, Hamamatsu City, Japan) or a 100× oil (NA 1.45) Plan Apochromat objective (Olympus) with an Eclipse Ti epifluorescence microscope (Nikon Instruments, Melville, NY) mounted with a Orca-Flash4.0 camera (Hamamatsu). Images were deconvolved using the Huygens deconvolution software (SVI), prepared with Fiji and assembled with Illustrator (Adobe).

Image analysis

Non-deconvolved *z*-stack images were projected using a maximum intensity projection method (Fiji). A modified version of CellProfiler (version 1.0.5122) (Carpenter et al., 2006) was used to analyse the dataset images. Global image thresholding using Otsu's method was applied to the DAPI channel to segment nuclei. Cyclin A nuclear intensity was determined by subtracting the median pixel value of the expanded segmented nuclear area edge, corresponding the local background signal, from the median pixel value of the shrunken segmented nuclear area. Centromere detection was performed using the A-Trous Wavelet transform algorithm applied to the CREST channel. Each centromere detected was affiliated to the segmented nucleus according to their coordinates. We developed a library of in-house MATLAB scripts (version R2011b, MathWorks) that allow us to extract in an automated fashion values from the CellProfiler MATLAB files. The centromeric fluorescent signal was determined by subtracting the median pixel value from the edge of a 7-pixel wide circle centred on the detected centromere, corresponding to the local background signal, from the maximum pixel value of a 3-pixel wide circle centred on the same detected centromere. For the CENP-A maintenance assay, the brightest 30% of centromeres were used for quantification. The CENP-A loading assay results were assessed by manually counting by visual inspection from three independent experiments.

Cell fractionation, western blot and antibodies

For cell fractionation, cells were harvested by trypsinization and washed with cold PBS. Cytosol and nuclei were extracted using the NE-PER extraction kit (Pierce, Thermo Fisher, Rockford, USA). Nucleoplasm and chromatin were subsequently extracted by sucrose cushion centrifugation after lysis of the nuclei in 100 mM KCl, 10 mM Hepes (pH 7.7), 50 µM sucrose, 0.25% Triton X-100 and with addition of various inhibitors (inhibitor cocktail, Roche; NaF; β-glycerophosphate; Leupeptin; Pepstatin; PMSF). Cell lysate preparations were applied to SDS-PAGE gels and proteins were transferred onto PVDF membranes. Immunoreactive bands were visualized with enhanced chemiluminescence. The following antibodies were used: mouse anti-CENP-A (1:1000, Abcam), rabbit anti-RBBP7 (1:1000, Abcam), mouse anti-RBBP4 (1:1000, Abcam), mouse anti-GAPDH (1:2000, Sigma), rabbit anti-HJURP (1:1000) (Foltz et al., 2009), mouse anti-DDB1 (1:1000; BD Biosciences, San Jose, CA), rabbit anti-CUL4A (1:1000) (Olma et al., 2009), mouse anti-RPA (1:2000, Imgenex, Novus Biologicals, Littleton, CO), mouse anti-α-tubulin (1:10,000, Sigma), mouse anti-histone H3 (1:1000, Upstate, Merck) and peroxidase-conjugated goat anti-mouse or anti-rabbit IgG (1:5000, Pierce) antibodies.

Flow cytometry and BrdU labelling

Cells were collected by trypsinization, ixed in 70% ethanol overnight at −20℃, washed in PBS 0.25% Triton X-100 and blocked for 30 min in PBS 5% FCS 0.25% Triton X-100. Immunostaining was performed after 1 h incubation with rabbit anti-phosphorylated Ser10 histone H3 (1:50, Upstate) at room temperature, followed by 30 min incubation with conjugated anti-rabbit IgG Alexa 488 (1:500, Invitrogen). Cells were resuspended for 30 min at 37℃ in 50 µg/ml propidium iodide, 20 µg/ml ribonuclease and 38 mM Na_3Citrate (pH 7.5) solution. Flow-cytometry was performed with a FACScalibur flow cytometer (BD Biosciences) using CellQuest software. Data analysis was performed using FlowJo software. For assessing cell proliferation by BrdU labelling, cells were incubated in culture media supplemented with 30 µM 5-Bromo-2′-Deoxyuridine (BrdU, Sigma) for 30 min and washed twice with culture media. After 16 h, cells were harvested, fixed and incubated in 2 M HCl containing 0.5% Triton X-100 for 30 min at room temperature. 0.1 M sodium tetraborate (Sigma) was then added and cells were washed with PBS containing 1% BSA (BSA, Fraction V, Roche) before staining with conjugated anti-BrdU FITC antibody (1:100, eBioscience, San Diego, CA). DNA labelling, data acquisition and analysis were performed as described.

Pull downs and immunoprecipitation

Transiently transfected HeLa 'Kyoto' cell lines were collected from tissue culture plates by scraping in lysis buffer [10 mM Tris-HCl pH 8, 100 mM KCl, 2 mM $MgCl_2$, 0.5% NP-40, 300 mM sucrose, 10 mM β-glycerophosphate, 0.2 mM NaF, 0.2 mM PMSF, 0.5 mM DTT, leupeptine, protease inhibitors mix (Roche) and nuclease (Pierce)] and cells were lysed by several passage through a 27G needle on ice. Cell lysates were centrifuged at 11,000 ***g*** for 15 min at 4℃, and cleared supernatant was applied to non-reactive agarose resins for 10 min at 4℃ to reduce non-specific binding to resins. The protein concentration of the

pre-cleared supernatants was measured by a Bradford assay, and equal amounts of protein were applied to anti-HA-coupled agarose resin (clone HA-7, Sigma) for 2 h at 4℃. Elution was performed using 100 mM glycine (pH 2) and eluates were neutralized by addition of ammonium bicarbonate. To immunoprecipitate endogenous CUL4A, HeLa 'Kyoto' cells were lysed as described above and incubated with Affi-Prep Protein A Support resin (Biorad). Rabbit IgG and rabbit anti-CUL4A antibodies (Olma et al., 2009) were incubated for 1 h at room temperature and were subsequently washed extensively with 0.2 M sodium tetraborate pH 9 (Sigma) before chemical cross-linking using 20 mM dimethyl pimelimidate (Sigma) for 30 min followed by extensive washes with 250 mM Tris-HCl (pH 8). Pre-cleared cell lysates were incubated 20 min at 4℃ with cross-linked resins, and elution was performed as described above using 100 mM glycine (pH 2).

Handling of insect cells, protein expression and pull-down assays

Insect cell lines were grown in suspension in SF-900 II SFM medium (Invitrogen) in a humidified incubator at 27℃ under constant shaking. RBBP7 and RBBP4 complete open reading frames were cloned into pFastBac Dual vectors (Invitrogen) containing either an N- or C-terminal Strep tag. Bacmids were produced in DH10Bac/Multibac *E. coli* bacterial strains and extracted according to manufacturer's instructions. Log-phase Sf-9 cell lines (Invitrogen) were transformed with Bacmid DNA using Cellfectin II (Invitrogen) according to the manufacturer's instructions. Strep-tagged RBBP7 and RBBP4 viruses were amplified after successive rounds of infections. Viruses for His–DDB1 infection were a kind gift of Nicolas H. Thomä (Scrima et al., 2008). Protein expression for pull-downs was performed after co-infection of High Five cells (Invitrogen). Infected cells were lysed by sonication in cold extraction buffer (50 mM Tris-HCl pH 8, 250 mM NaCl, 4 mM $MgCl_2$, 0.5% NP-40, 5% glycerol, 2 mM ATP, 2 mM DTT, 1 mM PMSF, benzonase, benzamidine, proteases inhibitor mix, Roche). Lysates were centrifuged at 12,000 ***g*** for 30 min at 4℃, and pre-cleared supernatant was applied to magnetic beads for 1 h at 4℃. M-280 Streptavidin dynabeads (Invitrogen) or TALON dynabeads (Invitrogen) were used for Strep- or His-tag pulldown assays, respectively. $CRL4A^{RBBP7}$ and $CRL4B^{RBBP7}$ complexes harbouring a FLAG-tag fused to the N-terminus of the respective CUL4 subunit were expressed from a single vector (pFL MultiBac) in Sf-9 cells. The cell pellets were resuspended in lysis buffer [50 mM Tris-HCl pH 7.5, 350 mM NaCl, 1 mM EDTA, 0.5% Triton-X, 1 mM DTT, protease inhibitor cocktail (Roche)] and purified with M2 FLAG-affinity agarose (Sigma-Aldrich) for 1 h, gently rotating at 4℃. Subsequently, the resin was washed three times with lysis buffer and three times with wash buffer (50 mM Tris-HCl pH 7.5, 150 mM NaCl). Elution of CRL complexes was achieved by applying one resin volume of 3×FLAG peptide at final concentration of 2 mg/ml in wash buffer with 10% glycerol.

Statistical analysis

Lilliefors' composite goodness-of-fit test was applied to test normality of the datasets. A Wilcoxon rank sum test or paired two-sided Student's *t*-test was performed to compare datasets when appropriate. Statistical analyses were performed using MATLAB software (MathWorks). Standard deviation and standard error of the mean were calculated using Excel (Microsoft). Dataset sizes are indicated as '*n*'.

Note added in proof

After acceptance of this work for publication, it has come to the attention of the authors the recent work by Niikura et al. (2015), who report that CRL4 in complex with COPS8/CSN8 is also required for CENP-A centromeric localization.

Acknowledgements

We thank D. Foltz (University of Virginia, USA), L. Jansen (IGC, Portugal) and N. Thomä (FMI, Switzerland) for sharing reagents; R. Aebersold and P. Picotti for providing access to MS equipment; J. Gerez and E. Milani for MS support; the ETH ScopeM facility for microscopy support; M. Unger and P. Horvath for help with MATLAB; S. Erhardt for sharing unpublished results; members of the Peter and Meraldi laboratories for helpful discussions; and W. Piwko and A. Smith for critical reading of the manuscript.

Competing interests

The authors declare no competing or financial interests.

Author contributions

J.M., S.G., M.G.M., F.L. and M.B. performed the experiments; J.M., S.G., M.G.M., F.L., P.M. and M.P. participated in the experimental design; and J.M., S.G. and M.P. wrote the paper.

Funding

Work in the Peter laboratory was supported by the Swiss National Science Foundation (SNF) [grant number 31003A_141148], an ERC senior award [ERC Rubicon 268930] and ETH Zurich (ETHZ) [grant number FEL01092]. P.M. was supported by the SNF [grant number 31003A_151256], the University of Geneva and the Louis-Jeantet Foundation. J.M. was supported by a Marie-Curie Actions Intra-European Fellowship [grant agreement number 225141] and an ETHZ Postdoctoral Fellowship. F.L. was supported by a postdoctoral fellowship from the Human Frontiers Science Foundation (HFSP) [grant number HFSP_LT000376/2014]. M.G.M. was supported by a Predoctoral grant of the SNF [grant number PDFMP3-124904].

Supplementary material

Supplementary material available online at
http://jcs.biologists.org/lookup/suppl/doi:10.1242/jcs.162305/-/DC1

References

Allshire, R. C. and Karpen, G. H. (2008). Epigenetic regulation of centromeric chromatin: old dogs, new tricks? *Nat. Rev. Genet.* **9**, 923-937.

Bade, D., Pauleau, A.-L., Wendler, A. and Erhardt, S. (2014). The E3 ligase CUL3/RDX controls centromere maintenance by ubiquitylating and stabilizing CENP-A in a CAL1-dependent manner. *Dev. Cell* **28**, 508-519.

Barnhart, M. C., Kuich, P. H. J. L., Stellfox, M. E., Ward, J. A., Bassett, E. A., Black, B. E. and Foltz, D. R. (2011). HJURP is a CENP-A chromatin assembly factor sufficient to form a functional de novo kinetochore. *J. Cell Biol.* **194**, 229-243.

Bassett, E. A., DeNizio, J., Barnhart-Dailey, M. C., Panchenko, T., Sekulic, N., Rogers, D. J., Foltz, D. R. and Black, B. E. (2012). HJURP uses distinct CENP-A surfaces to recognize and to stabilize CENP-A/histone H4 for centromere assembly. *Dev. Cell* **22**, 749-762.

Bergmann, J. H., Rodríguez, M. G., Martins, N. M. C., Kimura, H., Kelly, D. A., Masumoto, H., Larionov, V., Jansen, L. E. T. and Earnshaw, W. C. (2011). Epigenetic engineering shows H3K4me2 is required for HJURP targeting and CENP-A assembly on a synthetic human kinetochore. *EMBO J.* **30**, 328-340.

Biterge, B. and Schneider, R. (2014). Histone variants: key players of chromatin. *Cell Tissue Res.* **356**, 457-466.

Black, B. E., Jansen, L. E. T., Maddox, P. S., Foltz, D. R., Desai, A. B., Shah, J. V. and Cleveland, D. W. (2007). Centromere identity maintained by nucleosomes assembled with histone H3 containing the CENP-A targeting domain. *Mol. Cell* **25**, 309-322.

Blower, M. D., Sullivan, B. A. and Karpen, G. H. (2002). Conserved organization of centromeric chromatin in flies and humans. *Dev. Cell* **2**, 319-330.

Bodor, D. L., Rodríguez, M. G., Moreno, N. and Jansen, L. E. T. (2012). Analysis of protein turnover by quantitative SNAP-based pulse-chase imaging. *Curr. Protoc. Cell Biol.* **55**, 8.8.1-8.8.34.

Bodor, D. L., Valente, L. P., Mata, J. F., Black, B. E. and Jansen, L. E. T. (2013). Assembly in G1 phase and long-term stability are unique intrinsic features of CENP-A nucleosomes. *Mol. Biol. Cell* **24**, 923-932.

Carpenter, A. E., Jones, T. R., Lamprecht, M. R., Clarke, C., Kang, I. H., Friman, O., Guertin, D. A., Chang, J. H., Lindquist, R. A., Moffat, J. et al. (2006). CellProfiler: image analysis software for identifying and quantifying cell phenotypes. *Genome Biol.* **7**, R100.

Carroll, C. W., Silva, M. C. C., Godek, K. M., Jansen, L. E. T. and Straight, A. F. (2009). Centromere assembly requires the direct recognition of CENP-A nucleosomes by CENP-N. *Nat. Cell Biol.* **11**, 896-902.

Carroll, C. W., Milks, K. J. and Straight, A. F. (2010). Dual recognition of CENP-A nucleosomes is required for centromere assembly. *J. Cell Biol.* **189**, 1143-1155.

Dambacher, S., Deng, W., Hahn, M., Sadic, D., Fröhlich, J., Nuber, A., Hoischen, C., Diekmann, S., Leonhardt, H. and Schotta, G. (2012). CENP-C facilitates the recruitment of M18BP1 to centromeric chromatin. *Nucleus* **3**, 101-110.

Dunleavy, E. M., Roche, D., Tagami, H., Lacoste, N., Ray-Gallet, D., Nakamura, Y., Daigo, Y., Nakatani, Y. and Almouzni-Pettinotti, G. (2009). HJURP is a cell-cycle-dependent maintenance and deposition factor of CENP-A at centromeres. *Cell* **137**, 485-497.

Dunleavy, E. M., Almouzni, G. and Karpen, G. H. (2011). H3.3 is deposited at centromeres in S phase as a placeholder for newly assembled CENP-A in G_1 phase. *Nucleus* **2**, 146-157.

Ekwall, K. (2007). Epigenetic control of centromere behavior. *Annu. Rev. Genet.* **41**, 63-81.

Fachinetti, D., Folco, H. D., Nechemia-Arbely, Y., Valente, L. P., Nguyen, K., Wong, A. J., Zhu, Q., Holland, A. J., Desai, A., Jansen, L. E. T. et al. (2013). A two-step mechanism for epigenetic specification of centromere identity and function. *Nat. Cell Biol.* **15**, 1056-1066.

Fischer, E. S., Scrima, A., Böhm, K., Matsumoto, S., Lingaraju, G. M., Faty, M., Yasuda, T., Cavadini, S., Wakasugi, M., Hanaoka, F. et al. (2011). The molecular basis of CRL4DDB2/CSA ubiquitin ligase architecture, targeting, and activation. *Cell* **147**, 1024-1039.

Foltz, D. R., Jansen, L. E. T., Bailey, A. O., Yates, J. R., III, Bassett, E. A., Wood, S., Black, B. E. and Cleveland, D. W. (2009). Centromere-specific assembly of CENP-a nucleosomes is mediated by HJURP. *Cell* **137**, 472-484.

Han, J., Zhang, H., Zhang, H., Wang, Z., Zhou, H. and Zhang, Z. (2013). A Cul4 E3 ubiquitin ligase regulates histone hand-off during nucleosome assembly. *Cell* **155**, 817-829.

Hayashi, T., Fujita, Y., Iwasaki, O., Adachi, Y., Takahashi, K. and Yanagida, M. (2004). Mis16 and Mis18 are required for CENP-A loading and histone deacetylation at centromeres. *Cell* **118**, 715-729.

He, Y. J., McCall, C. M., Hu, J., Zeng, Y. and Xiong, Y. (2006). DDB1 functions as a linker to recruit receptor WD40 proteins to CUL4-ROC1 ubiquitin ligases. *Genes Dev.* **20**, 2949-2954.

Held, M., Schmitz, M. H. A., Fischer, B., Walter, T., Neumann, B., Olma, M. H., Peter, M., Ellenberg, J. and Gerlich, D. W. (2010). CellCognition: time-resolved phenotype annotation in high-throughput live cell imaging. *Nat. Methods* **7**, 747-754.

Hemmerich, P., Weidtkamp-Peters, S., Hoischen, C., Schmiedeberg, L., Erliandri, I. and Diekmann, S. (2008). Dynamics of inner kinetochore assembly and maintenance in living cells. *J. Cell Biol.* **180**, 1101-1114.

Hewawasam, G., Shivaraju, M., Mattingly, M., Venkatesh, S., Martin-Brown, S., Florens, L., Workman, J. L. and Gerton, J. L. (2010). Psh1 is an E3 ubiquitin ligase that targets the centromeric histone variant Cse4. *Mol. Cell* **40**, 444-454.

Hotton, S. K. and Callis, J. (2008). Regulation of cullin RING ligases. *Annu. Rev. Plant Biol.* **59**, 467-489.

Jansen, L. E. T., Black, B. E., Foltz, D. R. and Cleveland, D. W. (2007). Propagation of centromeric chromatin requires exit from mitosis. *J. Cell Biol.* **176**, 795-805.

Kato, T., Sato, N., Hayama, S., Yamabuki, T., Ito, T., Miyamoto, M., Kondo, S., Nakamura, Y. and Daigo, Y. (2007). Activation of Holliday junction recognizing protein involved in the chromosomal stability and immortality of cancer cells. *Cancer Res.* **67**, 8544-8553.

Kim, I. S., Lee, M., Park, K. C., Jeon, Y., Park, J. H., Hwang, E. J., Jeon, T. I., Ko, S., Lee, H., Baek, S. H. et al. (2012). Roles of Mis18α in epigenetic regulation of centromeric chromatin and CENP-A loading. *Mol. Cell* **46**, 260-273.

Lacoste, N., Woolfe, A., Tachiwana, H., Garea, A. V., Barth, T., Cantaloube, S., Kurumizaka, H., Imhof, A. and Almouzni, G. (2014). Mislocalization of the centromeric histone variant CenH3/CENP-A in human cells depends on the chaperone DAXX. *Mol. Cell* **53**, 631-644.

Lagana, A., Dorn, J. F., De Rop, V., Ladouceur, A.-M., Maddox, A. S. and Maddox, P. S. (2010). A small GTPase molecular switch regulates epigenetic centromere maintenance by stabilizing newly incorporated CENP-A. *Nat. Cell Biol.* **12**, 1186-1193.

Lee, J. and Zhou, P. (2007). DCAFs, the missing link of the CUL4-DDB1 ubiquitin ligase. *Mol. Cell* **26**, 775-780.

Loyola, A. and Almouzni, G. (2004). Histone chaperones, a supporting role in the limelight. *Biochim. Biophys. Acta* **1677**, 3-11.

Mchedlishvili, N., Wieser, S., Holtackers, R., Mouysset, J., Belwal, M., Amaro, A. C. and Meraldi, P. (2012). Kinetochores accelerate centrosome separation to ensure faithful chromosome segregation. *J. Cell Sci.* **125**, 906-918.

Mellone, B. G., Grive, K. J., Shteyn, V., Bowers, S. R., Oderberg, I. and Karpen, G. H. (2011). Assembly of Drosophila centromeric chromatin proteins during mitosis. *PLoS Genet.* **7**, e1002068.

Merlet, J., Burger, J., Gomes, J.-E. and Pintard, L. (2009). Regulation of cullin-RING E3 ubiquitin-ligases by neddylation and dimerization. *Cell. Mol. Life Sci.* **66**, 1924-1938.

Moree, B., Meyer, C. B., Fuller, C. J. and Straight, A. F. (2011). CENP-C recruits M18BP1 to centromeres to promote CENP-A chromatin assembly. *J. Cell Biol.* **194**, 855-871.

Moreno-Moreno, O., Medina-Giró, S., Torras-Llort, M. and Azorín, F. (2011). The F box protein partner of paired regulates stability of Drosophila centromeric histone H3, CenH3(CID). *Curr. Biol.* **21**, 1488-1493.

Müller, S. and Almouzni, G. (2014). A network of players in H3 histone variant deposition and maintenance at centromeres. *Biochim. Biophys. Acta* **1839**, 241-250.

Müller, S., Montes de Oca, R., Lacoste, N., Dingli, F., Loew, D. and Almouzni, G. (2014). Phosphorylation and DNA binding of HJURP determine its centromeric recruitment and function in CenH3(CENP-A) loading. *Cell Reports* **8**, 190-203.

Murzina, N. V., Pei, X.-Y., Zhang, W., Sparkes, M., Vicente-Garcia, J., Pratap, J. V., McLaughlin, S. H., Ben-Shahar, T. R., Verreault, A., Luisi, B. F. et al. (2008). Structural basis for the recognition of histone H4 by the histone-chaperone RbAp46. *Structure* **16**, 1077-1085.

Niikura, Y., Kitagawa, R., Ogi, H., Abdulle, R., Pagala, V. and Kitagawa, K. (2015). CENP-A K124 ubiquitylation is required for CENP-A deposition at the centromere. **32**, 598-603.

O'Connell, B. C. and Harper, J. W. (2007). Ubiquitin proteasome system (UPS): what can chromatin do for you? *Curr. Opin. Cell Biol.* **19**, 206-214.

Obuse, C., Yang, H., Nozaki, N., Goto, S., Okazaki, T. and Yoda, K. (2004). Proteomics analysis of the centromere complex from HeLa interphase cells: UV-damaged DNA binding protein 1 (DDB-1) is a component of the CEN-complex, while BMI-1 is transiently co-localized with the centromeric region in interphase. *Genes Cells* **9**, 105-120.

Ohzeki, J., Bergmann, J. H., Kouprina, N., Noskov, V. N., Nakano, M., Kimura, H., Earnshaw, W. C., Larionov, V. and Masumoto, H. (2012). Breaking the HAC Barrier: histone H3K9 acetyl/methyl balance regulates CENP-A assembly. *EMBO J.* **31**, 2391-2402.

Olma, M. H., Roy, M., Le Bihan, T., Sumara, I., Maerki, S., Larsen, B., Quadroni, M., Peter, M., Tyers, M. and Pintard, L. (2009). An interaction network of the mammalian COP9 signalosome identifies Dda1 as a core subunit of multiple Cul4-based E3 ligases. *J. Cell Sci.* **122**, 1035-1044.

Perpelescu, M., Nozaki, N., Obuse, C., Yang, H. and Yoda, K. (2009). Active establishment of centromeric CENP-A chromatin by RSF complex. *J. Cell Biol.* **185**, 397-407.

Pickart, C. M. (2004). Back to the future with ubiquitin. *Cell* **116**, 181-190.

Piwko, W., Olma, M. H., Held, M., Bianco, J. N., Pedrioli, P. G. A., Hofmann, K., Pasero, P., Gerlich, D. W. and Peter, M. (2010). RNAi-based screening identifies the Mms22L-Nfkbil2 complex as a novel regulator of DNA replication in human cells. *EMBO J.* **29**, 4210-4222.

Ranjitkar, P., Press, M. O., Yi, X., Baker, R., MacCoss, M. J. and Biggins, S. (2010). An E3 ubiquitin ligase prevents ectopic localization of the centromeric histone H3 variant via the centromere targeting domain. *Mol. Cell* **40**, 455-464.

Ray-Gallet, D., Woolfe, A., Vassias, I., Pellentz, C., Lacoste, N., Puri, A., Schultz, D. C., Pchelintsev, N. A., Adams, P. D., Jansen, L. E. T. et al. (2011). Dynamics of histone H3 deposition in vivo reveal a nucleosome gap-filling mechanism for H3.3 to maintain chromatin integrity. *Mol. Cell* **44**, 928-941.

Régnier, V., Vagnarelli, P., Fukagawa, T., Zerjal, T., Burns, E., Trouche, D., Earnshaw, W. and Brown, W. (2005). CENP-A is required for accurate chromosome segregation and sustained kinetochore association of BubR1. *Mol. Cell. Biol.* **25**, 3967-3981.

Ribeiro, S. A., Vagnarelli, P., Dong, Y., Hori, T., McEwen, B. F., Fukagawa, T., Flors, C. and Earnshaw, W. C. (2010). A super-resolution map of the vertebrate kinetochore. *Proc. Natl. Acad. Sci. USA* **107**, 10484-10489.

Saade, E., Mechold, U., Kulyyassov, A., Vertut, D., Lipinski, M. and Ogryzko, V. (2009). Analysis of interaction partners of H4 histone by a new proteomics approach. *Proteomics* **9**, 4934-4943.

Schuh, M., Lehner, C. F. and Heidmann, S. (2007). Incorporation of Drosophila CID/CENP-A and CENP-C into centromeres during early embryonic anaphase. *Curr. Biol.* **17**, 237-243.

Scrima, A., Konícková, R., Czyzewski, B. K., Kawasaki, Y., Jeffrey, P. D., Groisman, R., Nakatani, Y., Iwai, S., Pavletich, N. P. and Thomä, N. H. (2008). Structural basis of UV DNA-damage recognition by the DDB1-DDB2 complex. *Cell* **135**, 1213-1223.

Shuaib, M., Ouararhni, K., Dimitrov, S. and Hamiche, A. (2010). HJURP binds CENP-A via a highly conserved N-terminal domain and mediates its deposition at centromeres. *Proc. Natl. Acad. Sci. USA* **107**, 1349-1354.

Silva, M. C. C., Bodor, D. L., Stellfox, M. E., Martins, N. M. C., Hochegger, H., Foltz, D. R. and Jansen, L. E. T. (2012). Cdk activity couples epigenetic centromere inheritance to cell cycle progression. *Dev. Cell* **22**, 52-63.

Stellfox, M. E., Bailey, A. O. and Foltz, D. R. (2013). Putting CENP-A in its place. *Cell. Mol. Life Sci.* **70**, 387-406.

Sullivan, B. A. and Karpen, G. H. (2004). Centromeric chromatin exhibits a histone modification pattern that is distinct from both euchromatin and heterochromatin. *Nat. Struct. Mol. Biol.* **11**, 1076-1083.

Tagami, H., Ray-Gallet, D., Almouzni, G. and Nakatani, Y. (2004). Histone H3.1 and H3.3 complexes mediate nucleosome assembly pathways dependent or independent of DNA synthesis. *Cell* **116**, 51-61.

Walczak, C. E., Cai, S. and Khodjakov, A. (2010). Mechanisms of chromosome behaviour during mitosis. *Nat. Rev. Mol. Cell Biol.* **11**, 91-102.

Wang, J., Liu, X., Dou, Z., Chen, L., Jiang, H., Fu, C., Fu, G., Liu, D., Zhang, J., Zhu, T. et al. (2014). Mitotic regulator Mis18β interacts with and specifies the centromeric assembly of molecular chaperone HJURP. *J. Biol. Chem.* **289**, 8326-8336.

Westhorpe, F. G. and Straight, A. F. (2013). Functions of the centromere and kinetochore in chromosome segregation. *Curr. Opin. Cell Biol.* **25**, 334-340.

Zaidi, I. W., Rabut, G., Poveda, A., Scheel, H., Malmström, J., Ulrich, H., Hofmann, K., Pasero, P., Peter, M. and Luke, B. (2008). Rtt101 and Mms1 in budding yeast form a CUL4(DDB1)-like ubiquitin ligase that promotes replication through damaged DNA. *EMBO Rep.* **9**, 1034-1040.

Zasadzińska, E., Barnhart-Dailey, M. C., Kuich, P. H. J. L. and Foltz, D. R. (2013). Dimerization of the CENP-A assembly factor HJURP is required for centromeric nucleosome deposition. *EMBO J.* **32**, 2113-2124.